Comparison of transcriptional responses of three multidrug resistant model microorganisms, *Staphylococcus aureus* ATCC BAA-39, *Escherichia coli* ATCC BAA-196 and *Acinetobacter baumannii* ATCC BAA-1790, on exposure to iodine-containing nano-micelle drug FS-1

Ilya S. Korotetskiy,[1*] Sergey V. Shilov,[1] Tatyana V. Kuznetsova,[1] Aleksandr I. Ilin,1[1] Monique Joubert,[2] Setshaba Taukobong,[2] Oleg N. Reva[2*]

[1]Scientific Center for Anti-Infectious Drugs, Almaty, Kazakhstan

[2]Centre for Bioinformatics and Computational Biology; Department of Biochemistry, Genetics and Microbiology; University of Pretoria, Pretoria, South Africa

*Address correspondence to Ilya S. Korotetskiy, laeda81@gmail.com regarding experimental procedures and to Oleg N. Reva, oleg.reva@up.ac.za regarding genome assembly and bioinformatics

Running title: Transcriptional response to iodine nano-micelles.

Keywords: transcriptomics, *Escherichia coli*, *Staphylococcus aureus*, *Acinetobacter baumannii*, antibiotic resistance, iodine, nano-micelle

Abstract

Iodine is one of the oldest antimicrobial agents. Till now there have been no reports on development of resistance to iodine. Recent studies showed promising results on the application of iodine-containing nano-micelles, FS-1, against antibiotic resistant pathogens as a supplement to antibiotic therapy. The mechanisms of action, however, remain unclear. The aim of this study was to perform a systemic analysis of gene regulation and metabolic alterations in three phylogenetically distant reference strains from ATCC culture collection representing multidrug resistant pathogens associated with nosocomial infections: *Escherichia coli* BAA-196, *Staphylococcus aureus* BAA-39 and *Acinetobacter baumannii* BAA-1790. These cultures were treated in 5 min exposure to sublethal doses of the iodine-containing drug FS-1 applied in the late lagging and the mid of the logarithmic growth phases. Complete genome sequences of these strains were obtained in previous studies. Gene regulation was studied by total RNA extraction and Ion Torrent sequencing followed by mapping the RNA reads against the reference genome sequences and statistical processing of read counts using the DESeq2 algorithm. It was found that the treatment of bacteria with FS-1 profoundly affected the expression of many genes involved in central metabolic pathways; however, alterations of gene expression profiles were species-specific and depended on the growth phase when the drug was applied. Disruption of respiratory electron-transfer membrane complexes, increased penetrability of bacterial cell wall, osmotic and oxidative stresses leading to DNA damage were the major factors influencing the treated bacteria.

IMPORTANCE. Infections caused by antibiotic resistant bacteria threaten public health worldwide. Combinatorial therapy when antibiotics are administrated together with supplementary drugs improving susceptibility of pathogens to regular antibiotics is considered as a promising way to overcome this problem. An induction of antibiotic resistance reversion by the iodine-containing nano-micelle drug FS-1 was reported recently. This drug is currently under clinical trials in Kazakhstan against multidrug resistant

tuberculosis. The effect of iodine solutes on metabolic and regulatory processes in bacterial cells remain unexplored that precludes the effective application of iodine-containing antimicrobials in medicine. The current work provides an insight into gene regulation in antibiotic resistant bacteria treated with iodine-containing nanoparticles. Our expectation is that this study will shed light on unexplored bioactivities of iodine and the mechanisms of its antibacterial effect when applied in low concentrations. This knowledge will aid in future design of new drugs against antibiotic resistant infections.

Introduction

Iodine was discovered by French chemist Bernard Courtois in 1811. Since then it has been used as one of the most successful disinfectants, which antimicrobial activity has never been compromised by an acquired or natural resistance. The history of discovery and a comprehensive overview of the use of iodine in medicine was published in 1961 on the 150 anniversary of discovery of this chemical element [1]. Multiple chemical compounds of iodine were widely used in pharmacopoeia in XIX century and in the first half of XX century as a remedy of various germ-born infections. Iodine has, however, significantly lost its ground in medicine after the discovery of antibiotics by Alexander Fleming in 1928, which have revolutionized the field of the modern medicine making antibiotics the most significant tools in this field [2, 3]. Although originally developed for treating human infectious diseases, remarkable antimicrobial properties of antibiotics have spread them to a broad application in farming, agroindustry and aquaculture [4]. The misuse and overuse of antibiotics has led to a strong selective pressure, resulting in the survival and wide distribution of antibiotic resistant pathogens threatening the public health systems worldwide [2, 4]. Eventually, the situation with the antibiotic resistance and development of new antibiotics came to a global crisis as

the price of creation and introduction of new more-and-more complex antibiotics was growing while the time of emergence of bacteria resistant to these antibiotics after their first introduction to the practice was shrinking leaving no chance for pharmaceutical companies to gain any income [5-8]. An urgent need in principally new approaches to cope with the problem of antibiotic resistance, which include repurposing of abundant antimicrobials, is generally recognized [9, 10]. It is of great importance to devise new strategies that focus on limiting, redirecting and/or reversing the antibiotic resistance in bacterial.

Surprisingly, despite having used iodine in medicine for over 200 years, the effect of iodine and derivative compounds on metabolic processes and gene expression in living organisms remains basically unexplored except for numerous studies on iodine-rich thyroid hormones. A reason for this may be that iodine was used in medicine mostly for topical wound treatment or in composition of industrial disinfectants designed for a rapid eradication of germs leaving no time for the treated bacteria to respond to the treatment either by gene regulation or metabolic adaptation. Only recently, several works were published which demonstrated rather complex mechanisms of the action of iodine on eukaryotic cells, mostly in respect of its effect on tumour cells. It was shown that the application of Lugol's iodine solution (5% I_2, 10% KI) on breast cancer cells altered the expression of several genes involved in estrogen metabolism and estrogen cell response improving the anti-cancer therapy [11, 12]. The effect of iodine on the global transcriptional profile was explored on *Saccharomyces cerevisiae* [13], but there were no systemic studies on how the treatment of pathogenic bacteria with sublethal concentration of iodine may affect their virulence, antibiotic resistance and general metabolism. An interesting fact was published by Klebanoff in 1967 [14] on the release of iodinated organic substances by leukocytes at spotted infections that suggested a possible natural therapeutic effect of iodine in concentrations much lower than that in disinfectants.

This discovery had no continuation in any further studies probably because the iodine-based antimicrobials looked in the flourishing days of the antibiotic era as an unpromising archaic aftermath of the XIX century medicine. Post-antibiotic era calls us to reconsider previously abandoned anti-infection remedies [15].

Iodine-containing drugs seems to be a viable option to overcome the antibiotic resistance problem, since they have strong antimicrobial properties and no acquired resistance to iodine has been reported [16-18]. Molecular iodine is an effective mild and nontoxic Lewis acid catalyst [19] of great potential to synthesize various macromolecular complexes [20] that can easily penetrate cells of microorganisms [21] and pass through bi-lipid layers of cell membranes [11]. Since iodine can easily penetrate cell membranes, its application may be efficient against intracellular infections. This concept was implemented in a new drug, FS-1, developed as a new medicine against multidrug resistant tuberculosis [21, 22]. FS-1 contains iodine molecules and ions bound to dextrin/oligopeptide nano-micelles. General composition of FS-1 particles is shown below:

$$[\{(L_n\,(MeJ_3)^+)_y\,\{Me(L_m)J]^+{}_x\}\,(Cl^-)_{y+x+k}]$$

where L – dextrin-polypeptide ligand; Me – Li/Mg ions; *n*, *m*, *x*, *y* and *k* – variable integers ≥ 1. Molecular mass of the micelles is in the range of 30–300 kD.

FS-1 has passed both the preclinical and clinical trials (www.clinicaltrials.gov, accession number NCT02607449) and was approved in Kazakhstan as a supplementary drug to be administrated with common antibiotics used against multidrug resistant (MDR) and extensively drug resistant (XDR) tuberculosis. It was demonstrated that the application of FS-1 increased the susceptibility of the treated bacteria to antibiotics [22]; however, molecular

mechanisms of this action remain unclear. As the use of multidrug resistant *M. tuberculosis* isolates for further studies was technically challenged, the study of the action of iodine-containing nano-micelles on antibiotic resistant bacteria was continued using the ATCC collection strains: *Escherichia coli* BAA-196, *Staphylococcus aureus* BAA-39 and *Acinetobacter baumannii* BAA-1790. Complete genome sequences of these microorganisms were obtained using SMRT PacBio sequencing for two variants: the initial culture and the culture grown with sub-bactericidal concentrations of FS-1 in 10 daily passages [23-25]. Global genetic variations, epigenetic modifications and altered gene regulation in *E. coli* BAA-196 cultivated with FS-1 were analysed in recent publications [26, 27]. The aim of the current study was to perform a systemic analysis of gene expression and metabolic alteration in these three selected multidrug resistant pathogens affected by a 5 min exposure to the sublethal dose of the iodine-containing drug FS-1 in the late lagging and the mid of the logarithmic growth phases. Our expectation is that this study sheds light on unexplored bioactivities of iodine and that the comprehensive knowledge of metabolic and regulatory pathways affected by iodine-containing nano-micelles will aid in design of new drugs against multidrug resistant infections.

Results

The effect of 5 min exposure to FS-1 on gene expression was analysed on three model microorganisms: *E. coli* ATCC BAA-196, *S. aureus* ATCC BAA-39 and *A. baumannii* ATCC BAA-1790. Total RNA extracts were sequenced by the Ion Torrent technology. Then the RNA reads were mapped against the complete genome sequences of these microorganisms. The drug FS-1 was applied at the end of the lagging growth phase (Lag-experiment) and in the mid of the logarithmic growth phase (Log-experiment). Growth

curves estimated for the model microorganisms are shown in Supplementary Fig. S1. Each experiment was performed three or six times to allow estimation of statistical reliability of the results. Then the counts of reads overlapping individual genes were normalized by the program Bioconducter DESeq2 and statistical parameters of the differential gene expression were calculated. Involvement of the regulated genes in metabolic pathways was predicted by the program Pathway Tools and KEGG Pathway database.

Gene expression differences equal or higher than 2-folds with the estimated *p*-value equal or lower than 0.05 were considered as significant and statistically reliable. Numbers of up- and downregulated genes in the Lag and Log growth phases in three model microorganisms are shown in Table 1. Numbers of regulated genes and ratios of up- and downregulated genes varied in different species and growth phases. All regulated genes identified in *E. coli*, *S. aureus* and *A. baumannii* are listed in supplementary Tables S1, S2 and S3, respectively.

Despite the different numbers of differentially expressed genes, the gene regulation caused by the FS-1 treatment at different growth phases showed some level of co-regulation with Pearson correlation coefficients 0.504, 0.441 and 0.259 calculated at the Lag and Log experimental conditions respectively for *E. coli*, *S. aureus* and *A. baumannii* (Fig. 1). In the case with *A. baumannii*, the correlation was smaller due to an opposite regulation of several genes involved in taurine, sulphate and nitrate transportation (*tauAB*, *cysA*, *cysP*, *cysW*, *ybaN*), which were significantly downregulated by the treatment with FS-1 in the Lag growth phase but upregulated in the Log phase at the same condition. In *S. aureus*, an alternative regulation was observed for the gene *pyrC* involved in pyrimidine *de novo* biosynthesis.

Differential gene expression in *E. coli* ATCC BAA-196

Differential gene expression in *E. coli* treated for 5 min with FS-1 in the Lag and Log growth phases is shown in Supplementary Table S1. The scheme of regulated metabolic pathways is shown in Fig. 2.

The treatment with FS-1 has affected the central metabolism of the bacterium. All genes of the tricarboxylic acid cycle (TCA), *fumA*, *sdhA*, *sdhB*, *sucA*, *sucB* and *sucC*, were strongly downregulated at least in one growth phase. The glyoxylate shunt genes *acnB* and *gltA* were downregulated in the Log phase. Glycolytic gene *pfkA* was 3-fold upregulated in the Lag and Log experiments, while the fructose-1,6-bisphosphatases *fbp* and *glpX* participating in gluconeogenesis were 1.9-fold and 2.1-fold downregulated; however, this regulation was statistically unreliable ($p > 0.05$). In the Log-phase, these genes did not show any significant regulation but the glycolytic gene *tpiA* was 3-fold upregulated. All these observations indicate a general trend on activation of glycolysis over gluconeogenesis in the FS-1 treated *E. coli* [27]. The strong suppression of the TCA cycle with the upregulation of glycolysis are indicative for anaerobiosis [29]. A complete switch to anaerobiosis was reported for this strain cultivated for 10 passages with FS-1 as reported in the previous study [26]. In this study, a strong upregulation of NADH:quinone oxidoreductase *ndh* was observed in both growth phases. This enzyme is important for aerobic and anaerobic respiration. It participates in transportation of protons from NADH to oxygen through a cascade of H^+-transporting ubiquinol oxidases CyoABCD (these genes were insignificantly downregulated by FS-1) or CydABXH (insignificantly upregulated), or to nitrates through ubiquinol:nitrate oxidoredutases NarGHI (*narG* was 6.6-fold downregulated, $p = 0.09$). Mixed acid fermentation enzymes (*acnB*, *adhE*, *gltA*, *fdhF*, *frdA*, *frdB*) and all other electron transfer systems were mostly downregulated, namely: formate-to-dimethyl sulfoxide (DMSO)/nitrite/ trimethylamine N-oxide (*fdoGH*); glycerol-3-phosphate (G3P)-to-cytochrome *bo* oxidas

(*glpD*); G3P-to-fumarate/hydrogen peroxide reductases (*glpAB*, *frdA*); NADH/hydrogen-to-fumarate reductase (*frdA*) and succinate-to-cytochrome *bd* oxidase (*sdhAB*). An only exception was the upregulated NADH-to-DMSO electron transfer system catalysed by a complex of dimethyl sulfoxide reductase DmsABC with menaquinol. In Log-phase, *dmsB* was 8-fold upregulated. It suggests a possible transition of the FS-1 treated *E. coli* towards anaerobic respiration using DMSO as a terminal electron acceptor.

Many catabolic processes and almost all transmembrane transportation systems were inhibited, also. Downregulation was observed for the genes involved in carbohydrate transportation (*lamB*, *malE*, *malK*, *mglABC*, *treB*) and degradation (*fruK*); acetate/glycolate permease *actP*, galactitol transportation and degradation (*gatYZ*); cyanate transportation and degradation (*cynS*, *cynT*, *cynX*); glycerol and glycero-phosphodiester degradation (*glpABDKO*, *dhaKL*); propionate degradation through 2-methylcitrate cycle (*acnB*, *acs*, *fadD*), pyrimidine and deoxyribose degradation (*deoAC*); fatty acid transportation (*fadL*) and fatty acid beta-oxidation by the aerobic (*fadBDE*) and anaerobic (*fadIJ*) pathways. Several anabolic pathways were activated including the fatty acid, lipid and lipopolysaccharide biosynthesis (*accD*, *lpxA*, *rfaD*); peptidoglycan synthesis and recycling (*glmS*, *spr*); synthesis of polyamines (*speB*); nucleotide and histidine biosynthesis (*guaB*, *nrdA*, *thyA*); and porphyrin synthesis from glutamate (*hemL*). Synthesis and degradation of amino acids remained either unaffected or inhibited. Genes encoding multiple ribosomal proteins (*rimM*, *rplI*, *rplL*, *rplU*, *rpsT*, *rpsU*, *rpmA*, *yfgB*) and the protein translation/maturation genes (*efp*, *fklB*) were significantly upregulated that may indicate an increased protein synthesis. The activated anabolism combined with the inhibition of the nutrient uptake systems may lead to the starvation stress and general catabolic repression controlled by the (p)ppGpp alarmone system that is activated by increased concentration of uncharged tRNA [30]. To prevent the

stringent response, the genes encoding multiple tRNA charging enzymes (*argS*, *glnS*, *glyQ*, *glyS*, *tyrS*) and *spoT* ppGpp hydrolase were upregulated [31] by the treatment with FS-1.

The regulatory network of differential gene expression in the FS-1 treated *E. coli* was modelled by the program PheNetic (Fig. 3). Differentially expressed genes belonged to several regulons controlled by the DNA-binding transcriptional dual regulators CRP, FNR and ArcA, which are involved in the transition from aerobic to anaerobic growth; and also by three interdependent stress-response sigma-factors, RpoE, RpoS and RpoH, and the osmotic/heavy metal stress response DNA-binding transcriptional regulator CueR. The latter regulator controls expression of the copper transporter CopA and multicopper oxidase CueO, which were significantly upregulated in the FS-1 treated *E. coli*. CRP regulator acts mostly as a transcriptional repressor activated by cAMP in response to the osmotic stress [32-34]. Also, it was reported that cAMP-CRP complex regulates the central metabolism and carbon source utilization under unavailability of glucose [35].

Differential gene expression in *S. aureus* ATCC BAA-39

Gene regulation in *S. aureus* treated with FS-1 in the Lag and Log growth phases is shown in Supplementary Table S2. The scheme of regulated metabolic pathways is shown in Fig. 4.

The treatment with FS-1 suppresses TCA pathway (the genes *icd*, *sucC*) and activates glycolysis (*gpmI*, *pgk*, *tpiA*). This may indicate a possible transition to anaerobiosis [29]; however, the *cydA* gene encoding cytochrome *bd*-I ubiquinol oxidase involved in oxidative phosphorylation process is significantly activated in the FS-1 treated *S. aureus*. Cytochrome *bd*-I terminal oxidase catalyses reduction of NADH molecules by molecular oxygen or oxygen rich compounds such as nitrates and nitrites. The genes *nirB* and *narGH* encoding

nitrite/nitrate reductases involved in the dissimilatory nitrite reduction for anaerobic respiration were significantly upregulated in the FS-1 treated *S. aureus*. Another upregulated gene related to anaerobiosis is *fnt* encoding bidirectional formate-nitrite transporter. Fnt plays an important role in regulation of the level of intracellular formate during anaerobic respiration and in providing intracellular dissimilatory nitrite reductases with nitrite. Activation of this transporter may be a preparatory step for anaerobiosis as the key enzyme of the anaerobic metabolism, pyruvate:formate lyase PflB that coverts pyruvate to acetyl-CoA and formate, was downregulated in the treated *S. aureus*. Acetyl-CoA synthesis from acetate is activated by upregulation of the acetate kinase *ackA*. However, this enzyme may work in the opposite direction and can catalyse ATP production from acetyl-CoA. One of the major sources of acetyl-CoA in cells is beta-oxidation of fatty acids. This pathway was inhibited in the FS-1 treated *S. aureus* (Lag-phase experiment) by downregulation of the genes *fadA* (2.5-fold, p = 0.2) and *fadB* (7.5-fold, $p = 0.07$). Contrary, fatty acid biosynthetic enzyme acetyl-CoA carboxyltransferase *accD* was 1.7-fold upregulated. All these genes were not regulated in the Log-phase experiment. The analysis of the gene expression pattern suggests that *ackA* was activated for acetyl-CoA production. Also, this gene plays an important role for *S. aureus* in maintenance of metabolic homeostasis at stressful conditions [36].

Amino acid metabolism was generally downregulated in the FS-1 treated culture except for the glutamate biosynthesis via glutamine (*glnA*, *gltD*) followed by porphyrin biosynthesis (*hemC*) that in *S. aureus* is associated with the growth in anaerobic conditions [37]. Activated synthesis of menaquinone by upregulation of the genes *menD* and *menH* also may be associated with anaerobiosis as the encoded compounds are parts of the NADH:menaquinone electron transfer system controlled by NDH oxidoreductase [38]. The respective gene *ndh2* was 1.8-fold upregulated in the Lag-phase experiment ($p = 0.5$).

De novo purine (*purA*) and pyrimidine (*pyrG*, *thyA*) biosynthesis and salvage (*guaC*) genes were activated in the Lag-phase experiment as well as the xanthine permease *pbuX* and the hypoxanthine/guanine permease *pbuG*, while the uracil:proton symporter *pyrP* was strongly downregulated. The gene *deoB* associated with nucleotide degradation was downregulated. DNA repair proteins were differentially regulated. The methyl-directed mismatch repair complex *mutSL*, modified pyrimidine reparative endonuclease *nth*, UV DNA repair and Holliday junction renaturation helicases *pcrA* and *ruvB*, RNA decay controlling helicase *cshB*, negative supercoil relaxase *topA*, superoxide dismutase *sodA* and DNA recombination gene *radA* were strongly upregulated. Contrary, the SOS-response genes *recA*, *lexA* and *uvrAB* responsible for the repair of double-strand DNA breaches were downregulated.

Many genes controlling the accuracy of protein synthesis were activated in the FS-1 treated *S. aureus*. These genes involve the tRNA charging (*aspS*, *gltX*, *hisS*, *ileS*, *leuS*, *pheS*, *valS*) and tRNA processing (*gatA*, *gatC*, *miaB*) genes, genes for ribosomal proteins (*rimM*, *rlmB*, *rplJ*, *rpmG*, *rpmH*, *rpsP*, *yjbO*), RNA transcription terminator *rho*, protein release factor *prfC*, protein translocase *secG* and transpeptidase-transglycosylase *sgtA*. Contrary, the ribosomal inhibitor *raiA*, ribosomal methyltransferases *mraW* and *rlmH*, and protein uptake translocase *secA2* were downregulated. The chaperon encoding genes, *copZ*, *dnaJ*, *dnaK*, *groL* and *hslO*, were significantly upregulated.

In contrast to *E. coli*, transmembrane transportation proteins generally were not suppressed by the treatment with FS-1. The branched chain amino acid transporter *brnQ*, amino acid permease *lysP2*, cysteine transporter *tcyAB* and histidine transporter *yuiF* were upregulated, while D-serine/D-alanine/glycine transporter *cycA1*, glutamine transporter *glnQ* and amino acid permease *gabP* were downregulated. Carbohydrate, organic acid and fatty acid transporters *fruA* (fructose), *scrA* (sucrose), *lctP2* (L-lactate) and *msbA* (lipids) were activated

while the mannitol transporter *mtlA*, oligopeptide transporters *oppA2*, *oppD* and *oppF3*, trehalose transporter *treP* and choline transporters *opuBA* and *opuBB* were inhibited. The multidrug resistance efflux pump *norA*, multiple heavy metal efflux pumps (*copA*, *czrA*, *mntH*, *nikE*, *zitB*), putative sugar efflux transporter HMPRNC0000_0740 and auxin efflux transporter HMPRNC0000_2472 were upregulated.

Transporters of inorganic solutes were significantly activated. These systems include the iron and siderophore uptake genes *ceuB* and *sirA*, an operon of iron compound ABC uptake transporter permeases HMPRNC0000_0811-0813 and the ferrichrome-binding periplasmic protein HMPRNC0000_2507. Various Na^+-symporters, *kefC*, *mnhC*, *mnhD*, *nhaC* and HMPRNC0000_0689; as well as K^+-uptake proteins (*ktrA* and *ntpJ2*) and alkanesulfonate transporter *ssuC* were activated. Potassium transport system Ktr plays an important role in the maintenance of the osmotic homeostasis in *S. aureus* [39]. Other osmoprotective compounds, glycine betaine and polyamines, were synthesized (*betB*) or transported to the cell (*opuD2*, *potA*, *potC*). Osmotic stress may be caused due to damaging of the bacterial cell wall by iodine. Genes involved in cell wall biosynthesis were regulated differentially. The peptidoglycan synthesis, salvage and stress response genes, N-acetylmuramoyl-L-alanine amidase *atl*, peptidoglycan DD-endopeptidase *dacB*, cell wall stress response autolysin *amiD2* and cell wall biosynthesis genes *fmtB2*, *murD* and *murE* were upregulated. Contrary, the D-alanylalanine ligase *ddl*, peptidoglycan transglycosylase *mgt*, N-acetylmuramic acid 6-phosphate etherase *murQ* and N-acetylmuramic acid-specific transporter *sacX* were downregulated.

Differential gene expression in *A. baumannii* ATCC BAA-1790

Gene regulation in *A. baumannii* treated with FS-1 in the Lag and Log growth phases is shown in Supplementary Table S3. The scheme of regulated metabolic pathways is shown in Fig. 5.

In contrast to the previous two bacteria, the exposure of *A. baumannii* for 5 min to FS-1 did not affect transcription of genes encoding glycolysis/gluconeogenesis and TCA enzymes. Cytochrome *bd*-I terminal oxidase CydAB which showed upregulation in FS-1 treated *E. coli* and *S. aureus*, was suppressed in the FS-1 treated *A. baumannii*. In the text above it was hypothesized that the activation of this cytochrome complex together with the TCA downregulation and the activation of glycolysis might be indicative for the transition of bacteria to anaerobic respiration that possibly was not the case with the FS-1 treated *A. baumannii*. The aerobic fatty acid oxidation pathway was upregulated (*fadAB*) while the anaerobic branch of this pathway (*fadK*) was downregulated. No activation of any fermentation pathways or porphyrin biosynthesis was observed in the FS-1 treated *A. baumannii*. Many other metabolic pathways were regulated oppositely in the FS-1 treated *A. baumannii* compared to the treated *E. coli* and *S. aureus*. For example, glyoxylate pathway was activated by upregulation of the isocitrate lyase *aceA* and citrate synthase *gltA-2*. The genes associated with the synthesis of branched chain amino acids (*ilvHI*, *leuBCD*), aromatic amino acid (*aroF*), cysteine (*cysD*, *cysI*, *cysN*), arginine (*argG*), glutamate (*gltD*), methionine (*metB*) and S-adenosylmethionine (*metK*, *mmuM*) were upregulated at least in the Log-phase, while the ammonia-producing arginine catabolism genes (*astA*, *astB*, *astD*, *astE*) were downregulated. The treatment of *A. baumannii* with FS-1 has activated the ribosomal inhibitors *rsfA* and *yfiA* while the pattern of upregulated and downregulated ribosomal proteins was dissimilar to that in the FS-1 treated *E. coli* and *S. aureus* with many of these genes being strongly downregulated. The genes *pyrH*, *lpxH* and *fabF* involved in nucleotide

and fatty acid biosynthesis were downregulated while the nucleotide degradation and salvage genes *ppnP* and *rutF* were upregulated. A strong downregulation was observed for the potassium uptake proteins KdpABCD, which play an important role in maintenance of osmotic homeostasis [40, 42]. These genes were strongly upregulated in *E. coli* cultivated with FS-1 for 10 passages [26]. It may suggest that the cell-wall structures of *A. baumannii* were less affected by iodine and better protected the cells from the osmotic stress. However, the peptidoglycan synthesis and assembly genes *murI* and *dacA*, and the heavy metal resistance genes *copA* and *spxA* were strongly upregulated in FS-1 treated *A. baumannii* as it was observed in the FS-1 treated *E. coli* and *S. aureus*.

The activation of many genes involved in the thioredoxin pathway, glutathione-glutaredoxin redox reactions and oxidative stress response (*gntY*, *nfnB*, *usg*, *nemA*, *osmC* and *wrbA-2*) suggests that the FS-1 treated culture of *A. baumannii* experienced an oxidative stress. In the FS-1 treated *E. coli* and *S. aureus*, the homologous genes were not regulated, while other genes controlling the redox homeostasis were even downregulated: *grxA* and *trxC* in *E. coli*; *gpo* and *osmC* in *S. aureus*.

Multiple genes involved in iron scavenging and uptake were activated in the FS-1 treated *A. baumannii*, while the gene for iron storage bacterioferritin *bfr-1* was downregulated. The sulphate and thiosulphate uptake and assimilation genes (*cysA*, *cysB*, *cysP*, *cysW* and *cysU*) were strongly upregulated in the Log-phase that probably was associated with an activated biosynthesis of sulphate-containing amino acids cysteine, methionine and S-adenosylmethionine. The same was true for upregulation of the genes *tauAB* controlling the uptake and assimilation of sulphate-rich compound taurine. The nitrate/sulfonate/bicarbonate ABC transporter *ybaN* collocated on the chromosome with the *tauAB* operon was also activated. In the Lag-phase, all these genes were strongly downregulated. Contrary, the

phosphate ABC transporter permease subunits *pstA* and *pstB* were downregulated by the treatment with FS-1 in the Log-phase but upregulated in the Lag-phase. There were several other genes showing the opposite regulation in the Lag and Log experiments including the sigma factor *rpoH* and *merR* transcriptional regulator, which were upregulated by the treatment with FS-1 in the Lag-phase but downregulated in the Log-phase. Differential expression of these top-level transcriptional regulator may be behind the opposite regulation of other genes in the Lag and Log experiments.

Transcriptional regulation of the genes located on the plasmids of *E. coli* ATCC BAA-196 and *A. baumannii* ATCC BAA-1790

Genomes of the two model microorganisms used in this study, *E coli* and *A. baumannii*, comprise plasmids of 266,396 bp and 67,023 bp, respectively. There are 264 predicted protein coding genes on the *E. coli* plasmid, but almost all of them were transcriptionally silent at the experimental and negative control conditions. A rudimental transcription was recorded only for 8 transposases, two beta-lactamases and two aminoglycosidase acetyltransferases. The treatment of these bacteria with FS-1 in the Lag-phase suppressed the transcription from all these genes and they showed a differential regulation in the Log growth phase. However, the observed changes in the level of gene expression in both experiments were statistically unreliable with *p*-values much higher than 0.05. A previously published study, where the *E. coli* BAA-196 strain was cultivated with FS-1 for 10 passages, showed a significant expression from almost all genes located on the plasmid, suggesting its importance in protection of this bacterium from environmental stresses [26]. Possibly, the five-minutes treatment with FS-1 was insufficient for the plasmid activation.

The *A. baumannii* plasmid comprises 82 protein coding genes. Almost all these genes showed an expression when the strain was grown on the normal medium. Many of these genes were differentially regulated by FS-1. The highest level of up- and downregulation was observed for the genes encoding plasmid conjugation proteins. However, in all these cases the observed differential gene expression was statistically unreliable due to significant variations in the level of expression of these genes in three repeats of the experiment.

Comparison of the gene expression profiles of three model microorganisms treated with FS-1

To compare the patterns of gene expression, the program GET-HOMOLOGOUS [40] was used to identify homologous genes shared by the model microorganisms. A summary of this search is represented by Venn diagram on Supplementary Fig. S2. There were 504 genes shared by the three genomes and additionally 839 genes were common for *E. coli* and *A. baumannii*; 221 homologs were shared by *E. coli* and *S. aureus*; and more 122 homologous genes were shared by *S. aureus* and *A. baumannii*.

Plots of gene expression fold changes determined for homologous genes in pairs of model organisms, A) *E. coli* and *S. aureus*; B) *E. coli* and *A. baumannii*; C) *S. aureus* and *A. baumannii*; all treated with FS-1 in the Lag-phase, are shown in corresponding parts of Fig. 6. Calculated Pearson correlation coefficients were in the range from 0.044 for the pair *S. aureus* — *A. baumannii* (Fig. 6C) to 0.225 for the pair *E. coli* — *S. aureus* (Fig. 6A). Only one gene was found that had showed a significant upregulation in all three tested microorganisms. It was the heavy metal (copper, lead, cadmium, zinc and mercury) transporter *copA*. It suggests that the treatment with FS-1 increased penetrability of cells for

heavy metal ions in all tested bacteria probably due to damaging the cell wall molecules and structures. In response to the heavy metal ion influx, the corresponding efflux pumps were activated. This finding agrees with other study reporting disintegration of bacterial membranes by iodine nanoparticles [18]. Other authors reported that the copper homeostasis systems may be activated in *E. coli* in anaerobic conditions associated with amino acid limitation [43].

The close-to-zero level of gene coregulation in these three phylogenetically distant bacteria treated with FS-1 may be explained by the fact that the regulation of similar metabolic processes often is carried out by up- and downregulation of different genes involved in the metabolic pathways. Indeed, the comparison of the affected metabolic pathways of all these bacteria (Fig. 2, 4 and 5) demonstrated a higher similarity in their responses to the treatment with FS-1. First commonality was that many transmembrane transporters of carbohydrates, amino acids, oligopeptides and oligosaccharides were inhibited in all three bacteria. FS-1 is a complex of iodine molecules bound to dextrin fragments and oligopeptides. Transporters of these compounds may be entrance points of iodine to the cells. This may explain the observed inhibition of these genes; however, the spectra of inhibited and activated transporters were different in the tested bacterial species. Sodium-proline symporter *putP* was downregulated in all three tested bacteria almost at all conditions (except for *E. coli* in Log-phase). Iron scavenging and uptake proteins were activated in *S. aureus* and *A. baumannii*, probably due to immobilizing of iron ions by iodine into an insoluble iodide; however, in *E. coli* the expression of these genes did not change. Other systems of transmembrane uptake and utilization of various compounds were regulated differentially in the tested bacteria.

Synthesis of cell wall compounds including peptidoglycan and lipids generally was upregulated. This observation again indicates that the prime target of the released iodine was

the cell wall and cell membrane structures that is in agreement with other studies [18, 21]. Various efflux pumps, especially heavy metal resistance proteins, were activated. Activation of synthesis and uptake of osmoprotective molecules (glycine betaine and polyamines) and the potassium uptake systems in *E. coli* and *S. aureus* suggests that these strains experienced osmotic stress caused by the treatment with FS-1. In *E. coli*, an important role in gene regulation under the experimental condition was played by cAMP-CRP signal transduction system (Fig. 3). Other pathways of gene expression regulation were utilized by *S. aureus* and *A. baumannii* in their response to the treatment with FS-1. Strong downregulation of adenylate cyclase *cyaA* in *S. aureus* suggests that cAMP may not play a role in the response to FS-1 by this bacterium. The effect of FS-1 on *A. baumannii* in the Log growth phase was characterized with a significant downregulation of many genes including several important transcriptional regulators, which suppression could be behind this negative effect on the general gene expression. These transcriptional regulators were EnvZ/OmrR two-component signal transduction system involved in osmoregulation [44], RstA response regulator of many intracellular processes [45], potassium-dependent KdpD regulator controlling K^+-homeostasis [46], iron uptake regulator *fur*, sigma factor-32 *rpoH* and transcriptional regulator *merR*.

Discussion

An interesting finding of this work was that the tested model microorganisms responded differently to the short-time (5 min) treatment with the iodine-containing nano-micelles. Noteworthy, the treatment of *E. coli* and *S. aureus* with FS-1 caused the transition of these bacteria to anaerobiosis. One possible reason for this reaction may be damaging of electron transportation systems using O_2 as the electron acceptor by I_2 molecules. This causes bacteria to look for alternative electron acceptors such as DMSO in the case with *E. coli* and

nitrates/nitrites in the case with *S. aureus*. In another study on *E. coli* BAA-196 cultivated for 10 passages with FS-1, a complete halt of the expression of the genes for the cytochrome *bo* terminal oxidase complex, *cyoA*, *cyoB*, *cyoC* and *cyoE*, was observed [27] that corroborates with the hypothesis that iodine may interfere with the system of transportation of electrons between cytochromes and oxygen. This transition to anaerobiosis caused by the treatment with FS-1 may be of practical importance. Both these bacteria, *E. coli* and *S. aureus*, may survive anaerobic or microaerophilic conditions; however, at the expense of a reduction of their virulence and antibiotic resistance [47].

Another reason for the transition to anaerobiosis may be an attempt to avoid the oxidative stress caused by iodine in the medium. Oxidative phosphorylation is a source of peroxide radicals, which aggravate the oxidative stress. This hypothesis is supported by the observation of a strong oxidative stress response in the FS-1 treated *A. baumannii*, which in contrast to *E. coli* and *S. aureus* did not show any signs of transition to anaerobiosis. Several other incongruent responses by *A. baumannii* to the treatment with FS-1 compared to two other microorganisms, such as the activation of glycolysis and downregulation of TCA and glyoxylate pathway in *E. coli* and *S. aureus* with no effect in *A. baumannii*; the downregulation of the aerobic fatty acid beta-oxidation in *E. coli* and *S. aureus* and upregulation of this pathway in *A. baumannii*; alternative regulation of porphyrin biosynthesis and amino acid metabolism; all of them may be attributed to the transition of *E. coli* and *S. aureus* to anaerobiosis with the absence of such response in *A. baumannii*. The gene expression profiles in *A. baumannii* under the effect of FS-1 differed in the Lag- and Log-phases with several genes involved in sulphur, nitrogen and phosphorus uptake being regulated oppositely in these two experiments.

The treatment of bacteria with the iodine-containing micelle drug FS-1 caused osmotic and oxidative stresses to bacterial cells. The osmotic stress was associated with damaging of surface, cell wall and cell membrane proteins leading to increased penetrability of bacterial cells to heavy metal ions and possibly to antibiotics. This effect was more apparent to *E. coli* and *S. aureus*. Possible damaging of cytochrome-ubiquinol terminal oxidases participating in aerobic respiration brought the FS-1 treated *E. coli* and *S. aureus* to anaerobiosis that alleviated to some extent the oxidative stress. However, the strong inhibition of multiple nutrient uptake-and-utilization systems in *E. coli* could lead this bacterium to a shortage of energy and nutrients. In *S. aureus*, accumulation of iodine in cytoplasm caused damaging of DNA and possibly RNA molecules that was apparent by the observed activation of DNA repair and nucleotide salvage systems. This activation of the DNA repair systems in response to the treatment with FS-1 was not observed in other two bacteria. Cell wall of *A. baumannii* cells was apparently the most resistant against iodine and prevented cells from iodine penetration into cytoplasm. However, this bacterium was under a stronger oxidative stress compared to the other two microorganisms.

Conclusion

A finding of this work was that the tested pathogenic bacteria responded differently to the treatment with the iodine-containing nano-micelles depending also on the growth phase when the drug was applied. One common mechanism was the activation of the efflux pump CopA that probably identifies damaging of cell wall structures in all treated bacteria leading to the osmotic stress. This information will be of importance for the development of new iodine-containing nano-micelle drugs against antibiotics resistant nosocomial infections represented in this study by the reference multidrug resistant strains, *E. coli*, *S. aureus* and *A. baumannii*,

obtained from the ATCC. Further studies will aim on testing the effect of iodine-containing compounds on a broader collection of antibiotic resistant nosocomial infection agents isolated in clinics in several recent studies [48, 49]. Although iodine is in the use by humankind as an antimicrobial disinfectant for more than two centuries, to our best knowledge till now there have been no published reports on the effect of iodine applied in low concentrations in nano-micelle complexes on the gene expression and metabolism of pathogenic bacteria.

Materials and methods

Bacterial cultures

Multidrug resistant strains *Staphylococcus aureus* subsp. *aureus* ATCC® BAA-39™, *Escherichia coli* ATCC® BAA-196™ and *Acinetobacter baumannii* ATCC® BAA-1790™ were obtained from the American Type Culture Collection (ATCC) and used as the model organisms for this study. Stock cultures were kept in a freezer at −80°C. Bacteria were cultivated on Mueller-Hinton (MH) liquid or solid media (Himedia, India) without antibiotics (*S. aureus* and *A. baumannii*) and in the medium supplemented with ceftazidime 10 μg/ml (*E. coli*) as recommended in the ATCC product sheet. Before the use in the experiments, the strains were twice passaged on MH medium.

Determination of growth rates

Overnight (24 hours) culture growth was adjusted by dilution with sterile water to 1×10^7 CFU/ml and inoculated into microarray plates with MH liquid medium. Plates were incubated at 37°C on 60 rpm shaker for 24 hours with optical density (OD) recording every

5 min by Multiscan Ascent spectrophotometer (Thermo, Finland). The growth curves were estimated based on the obtained series of OD values in three repeats by Baranyi and Roberts model implemented in the interactive DMFit application [50] as shown in Supplementary Fig. S1.

Treatment with FS-1

Bacterial inoculants were incubated at 37°C as follows: *E. coli* for 1 hour (the end of the lagging growth phase, termed Lag-experiment) and for 6 hours (the mid of the logarithmic growth phase, Log-experiment); *S. aureus* for 2.5 hours (Lag) and 9 hours (Log); and *A. baumannii* for 1 hour (Lag) and 10 hours (Log). Lag and Log growth phases were estimated based on the strain specific growth curves on MH medium (Supplementary Fig. S1). Thereafter, the experimental cultures were suplemented with FS-1 to achieve the final concentration of 450 μg/ml (for *S. aureus*) or 500 μg/ml (for *E. coli* and *A. baumannii*) that corresponded to the half of the minimal bactericidal concentrations of FS-1 estimated for these bacteria; whereas for the negative control samples, the same volume of physiological saline was added to the bacterial cultures. Cultures were incubated for 5 min at 37°C with shaking. Metabolic processes were stopped by adding the killing buffer (2.0 ml of 1 M Tris-HCl, pH 7.5; 0.5 ml of 1 M $MgCl_2$, 1.3 g of NaN_3; 997.5 ml of water) in the volume ratio 1:1 [51]. All experiments were performed in three-six repititions to achieve the necessary amount of the total RNA generated reads. Bacterial cells were collected for RNA extraction by centrifugation at 5,000 g for 10 min.

RNA Library Preparation and Sequencing

Total RNA samples were extracted from the cultures with the use of the RiboPure Bacteria Kit (Ambion, Lithuania) as instructed by the developer's guidelines. Afterwards, the quantity and quality of the extracted RNA was verified with the use of the NanoDrop 2000c spectrophotometer (Thermo Scientific, USA) at optical wavelengths 260 and 280 nm. Purification of the total RNA from ribosomal 16S and 23S RNA was carried out using the MICROBExpress Bacterial mRNA Purification Kit (Ambion, Lithuania) following the developer recommendations. Thereafter, the effectiveness of sample purification was determined on the Bioanalyzer 2100 (Agilent, Germany) with the RNA 6000 Nano LabChip Kit (Agilent Technologies, Lithuania).

The library preparation from the extracted RNA samples included an enzymatic fragmentation step with the use of the Ion Total RNA Seq kit V2. Thereafter, the Ion Xpress RNA-Seq Barcode 01-16 Kit was used for RNA fragment barcoding. RNA sequencing was then performed using the Ion 318 Chip Kit V2 on the Ion Torrent PGM sequencer (Life Technologies, USA).

Differential gene expression analyses

The differential gene expression was estimated using the R-3.4.4 software packages. Firstly, reference indices were built for each reference genome using the *buildindex* function available in the *Rsubreads* package (Bioconducter, www.bioconductor.org). For each bacterium, the obtained RNA fragments were aligned to the relevant reference genomes in FASTA formats (*S. aureus* ATCC BAA-39 NC [CP033505.1], *E. coli* ATCC BAA-196 NC [CP042865.1 for chromosome and CP042866.1 for plasmid], *A. baumannii* ATCC BAA-1790 [CP042841.1 for chromosome and CP042842.1 for plasmid]). Resulted read alignment files in BAM format were sorted using Samtools software package available from htslib

(www.htslib.org) and used for counting of reads overlapping predicted gene locations by using the *featureCounts* function and the relevant genome annotation files in GFF format. The R packages *DESeq2* (Bioconducter) and *GenomicFeatures* tools were then used for normalization of read counts and calculation of the differential gene expression statistics.

Metabolic pathway and regulatory network analyses

With the use of identified differentially expressed genes, metabolic pathways and reactions controlled by those genes were identified using the Pathway Tools software [52] and KEGG Pathway database (https://www.genome.jp/kegg/pathway.html). Networks of regulated genes were constructed using the Web based tool PheNetic [53] based on the regulation network designed for *E. coli* K12 [NC_000913. 2] and available from the PheNetic Web site. Pairs of homologous genes in the genomes K12 and BAA-196, and also the homologous genes shared by *S. aureus* BAA-39, *E. coli* BAA-196 and *A. baumannii* BAA-1790 were identified using the program GET_HOMOLOGUES with the parameters set by default [40]. Large admixed clusters of homologous phage-related integrases and transposases were considered as strain-specific genes and excluded from the transcription comparison. Venn diagram with numbers of shared genes is shown in Supplementary Fig. S2.

Statistical evaluations

All RNA sequencing experiments were performed in six (*S. aureus* and *A. baumannii*) or three (*E. coli*) repetitions. Genes showing 2-fold or greater expression difference with calculated *p*-value equal or smaller 0.05 were considered as significantly regulated. Pearson

correlation coefficients (C_p) of gene coregulation were calculated by Eq. 1 implemented in an in-house Python 2.7 script.

$$C_P = \frac{N\sum x_i y_i - \sum x_i \sum y_i}{\sqrt{\left(N\sum x_i^2 - (\sum x_i)^2\right)\left(N\sum y_i^2 - (\sum y_i)^2\right)}} \quad \text{Eq. 1}$$

where x_i and y_i are fold-change values estimated for every i's homologous gene, N – total number of shared homologous genes.

Data availability

Experimental and negative control RNA reads generated in this study are freely available from BioProject Web-sites of the reference genomes deposited at NCBI: *S. aureus* BAA-39 NC, PRJNA480363; *E. coli* BAA-196 NC, PRJNA557356; *A. baumannii* BAA-1790 NC, PRJNA557366.

References

1. Kelly FC. 1961. Iodine in Medicine and Pharmacy Sinceits Discovery – 1811-1961. Proc R Soc Med 54:831-836.

2. Abraham EP, Chain E, Fletcher CM, Florey HW, Gardner AD, Heatley NG, Jennings MA. 1992. Further observations on penicillin. 1941. Eur J Clin Pharmacol 42:3-9.

3. Munita JM, Arias CA. 2016. Mechanisms of Antibiotic Resistance. Microbiol Spectr 4:10.1128/microbiolspec.VMBF-0016-2015. doi:10.1128/microbiolspec.VMBF-0016-2015.

4. Barbosa TM, Levy SB. 2000. The impact of antibiotic use on resistance development and persistence. Drug Resist Updat 3:303-311. doi:10.1054/drup.2000.0167.

5. Nicolaou KC, Montagnon T. 2008. Molecules that changed the world. Weinheim, Wiley-VCH.

6. Zucca M, Savioa D. 2010. The Post-Antibiotic Era: promising developments in the therapy of infectious diseases. Int J Biomed Sci 6:77–86.

7. Laxminarayan R. 2014. Antibiotic effectiveness: balancing conservation against innovation. Science 345:1299-1301. doi:10.1126/science.1254163.

8. Ventola CL. 2015. The antibiotic resistance crisis: part 1: causes and threats. P T 40:277-283.

9. Bush K, Courvalin P, Dantas G, Davies J, Eisenstein B, Huovinen P, Jacoby GA, Kishony R, Kreiswirth BN, Kutter E, Lerner SA, Levy S, Lewis K, Lomovskaya O, Miller JH, Mobashery S, Piddock LJ, Projan S, Thomas CM, Tomasz A, Tulkens PM, Walsh TR, Watson JD, Witkowski J, Witte W, Wright G, Yeh P, Zgurskaya HI. 2011. Tackling antibiotic resistance. Nat Rev Microbiol 9:894-896. doi:10.1038/nrmicro2693.

10. McClure NS, Day T. 2014. A theoretical examination of the relative importance of evolution management and drug development for managing resistance. Proc Biol Sci 281:20141861. doi:10.1098/rspb.2014.1861.

11. Anguiano B, García-Solís P, Delgado G, Aceves Velasco C. 2007. Uptake and gene expression with antitumoral doses of iodine in thyroid and mammary gland: evidence that chronic administration has no harmful effects. Thyroid 17:851-859. doi:10.1089/thy.2007.0122.

12. Stoddard FR 2nd, Brooks AD, Eskin BA, Johannes GJ. 2008. Iodine alters gene expression in the MCF7 breast cancer cell line: evidence for an anti-estrogen effect of iodine. Int J Med Sci 5:189-196. doi: 10.7150/ijms.5.189.

13. Kitagawa E, Akama K, Iwahashi H. (2005). Effects of iodine on global gene expression in *Saccharomyces cerevisiae*. Biosci Biotechnol Biochem 69:2285-2293. doi:10.1271/bbb.69.2285.

14. Klebanoff SJ. 1967. Iodination of bacteria: a bacteriocidal mechanism. J Exp Med 126:1063-1078. PMID: 4964565.

15. Pogue JM, Marchaim D, Kaye D, Kaye KS. 2011. Revisiting "older" antimicrobials in the era of multidrug resistance. Pharmacotherapy 31:912-921. doi:10.1592/phco.31.9.912.

16. Banerjee M, Mallick S, Paul A, Chattopadhyay A, Ghosh SS. 2010. Heightened reactive oxygen species generation in the antimicrobial activity of a three component

iodinated chitosan-silver nanoparticle composite. Langmuir 26:5901-5908. doi:10.1021/la9038528.

17. Murdoch R, Lagan KM. 2013. The role of povidone and cadexomer iodine in the management of acute and chronic wounds. Physical Therapy Reviews 18:207-216. doi:10.1179/1743288X13Y.0000000082.

18. Viswanathan K, Babu DB, Jayakumar G, Raj GD. 2017. Anti-microbial and skin wound dressing application of molecular iodine nanoparticles. Materials Research Express 4:104003.

19. Dandia A, Gupta SL, Maheshwari S. 2014. Molecular iodine: mild, green, and nontoxic lewis acid catalyst for the synthesis of heterocyclic compounds, p. 277-327. *In* Ameta KL, Dandia A. (eds.), Green Chemistry: Synthesis of Bioactive Heterocycles. Springer, New Delhi, India.

20. Moulay S. 2013. Molecular iodine/polymer complexes. J Polymer Eng 33:389-443.

21. Ilin A, Kerimzhanova B, Yuldasheva G. 2017. Action mechanism of molecular iodine complex with bioorganic ligands, magnesium and lithium halogenides on human tuberculosis strain with multiple drug resistance. Journal of Microbial and Biochemical Technology 9:293-300.

22. Ilin AI, Kulmanov ME, Korotetskiy IS, Islamov RA, Akhmetova GK, Lankina MV, Reva ON. 2017. Genomic insight into mechanisms of reversion of antibiotic resistance in multidrug resistant *Mycobacterium tuberculosis* induced by a

nanomolecular iodine-containing complex FS-1. Front Cell Infect Microbiol 7:151. doi:10.3389/fcimb.2017.00151.

23. Joubert M, Reva ON, Korotetskiy IS, Shvidko SV, Shilov SV, Jumagaziyeva AB, Kenesheva ST, Suldina NA, Ilin AI. 2019. Assembly of complete genome sequences of negative-control and experimental strain variants of *Staphylococcus aureus* ATCC BAA-39 selected under the effect of the drug FS-1, which induces antibiotic resistance reversion. Microbiol Resour Announc 8:e00579-19. https://doi.org/10.1128/MRA.00579-19.

24. Korotetskiy IS, Joubert M, Taukobong S, Jumagaziyeva AB, Shilov SV, Shvidko SV, Suldina NA, Kenesheva ST, Yssel A, Reva ON, Ilin AI. 2019. Complete genome sequence of a multidrug-resistant strain, *Escherichia coli* ATCC BAA-196, as a model for studying induced antibiotic resistance reversion. Microbiol Resour Announc 8:e01118-19. doi: 10.1128/MRA.01118-19.

25. Korotetskiy IS, Joubert M, Magabotha SM, Jumagaziyeva AB, Shilov SV, Suldina NA, Kenesheva ST, Yssel A, Reva ON, Ilin AI. 2020. Complete genome sequence of a collection strain *Acinetobacter baumannii* ATCC BAA-1790 used as a model to study the antibiotic resistance reversion induced by the iodine-containing complexes. Microbiol Resour Announc 9:e01467-19. doi: 10.1128/MRA.01467-19.

26. Korotetskiy IS, Jumagaziyeva AB, Shilov SV, Kuznetsova TV, Suldina NA, Kenesheva ST, Ilin AI, Joubert M, Taukobong S, Reva ON. 2020. Differential gene expression and alternation of patterns of DNA methylation in the multidrug resistant strain *Escherichia coli* ATCC BAA-196 caused by iodine-containing nano-micelle

drug FS-1 that induces antibiotic resistance reversion. bioRxiv. doi: 10.1101/2020.05.15.097816.

27. Korotetskiy IS, Shilov SV, Reva ON, Kuznetsova TV, Jumagaziyeva AB, Akhmatullina NB, Ilin AI. 2020. Gene expression profiling of multi-drug resistant *E. coli* after exposure by nanomolecular iodine-containing complex. News Nat Acad Sci of the Republic of Kazakhstan 4:2224-5308. doi: 10.32014/2020.2519-1629.27.

28. Sabnis NA, Yang H, Romeo T. 1995. Pleiotropic regulation of central carbohydrate metabolism in *Escherichia coli* via the gene *csrA*. J Biol Chem 270:29096-29104. doi:10.1074/jbc.270.49.29096.

29. Kohler C, von Eiff C, Liebeke M, McNamara PJ, Lalk M, Proctor RA, Hecker M, Engelmann S. 2008. A defect in menadione biosynthesis induces global changes in gene expression in *Staphylococcus aureus*. J Bacteriol 190:6351-6364. doi:10.1128/JB.00505-08.

30. Rojiani MV, Jakubowski H, Goldman E. 1989. Effect of variation of charged and uncharged tRNA(Trp) levels on ppGpp synthesis in *Escherichia coli*. J Bacteriol 171:6493-6502. doi:10.1128/jb.171.12.6493-6502.1989.

31. Chatterji D, Ojha AK. 2001. Revisiting the stringent response, ppGpp and starvation signaling. Curr Opin Microbiol 4:160-165. doi:10.1016/s1369-5274(00)00182-x.

32. Landis L, Xu J, Johnson RC. 1999. The cAMP receptor protein CRP can function as an osmoregulator of transcription in *Escherichia coli*. Genes Dev 13:3081-3091. doi: 10.1101/gad.13.23.3081.

33. Huang L, Tsui P, Freundlich M. 1992. Positive and negative control of *ompB* transcription in *Escherichia coli* by cyclic AMP and the cyclic AMP receptor protein. J Bacteriol 174:664-670. doi: 10.1128/jb.174.3.664-670.1992.

34. Balsalobre C, Johansson J, Uhlin BE. 2006. Cyclic AMP-dependent osmoregulation of *crp* gene expression in *Escherichia coli*. J Bacteriol 188:5935-5944. doi: 10.1128/JB.00235-06.

35. Shimada T, Fujita N, Yamamoto K, Ishihama A. 2011. Novel roles of cAMP receptor protein (CRP) in regulation of transport and metabolism of carbon sources. PLoS One 6:e20081. doi: 10.1371/journal.pone.0020081.

36. Sadykov MR, Thomas VC, Marshall DD, Wenstrom CJ, Moormeier DE, Widhelm TJ, Nuxoll AS, Powers R, Bayles KW. 2013. Inactivation of the Pta-AckA pathway causes cell death in *Staphylococcus aureus*. J Bacteriol 195:3035-3044. doi: 10.1128/JB.00042-13.

37. De la Fuente R, Schleifer K.H., Götz F, Köst H.-P. 1986. Accumulation of porphyrins and pyrrole pigments by *Staphylococcus aureus* ssp. *anaerobius* and its aerobic mutant. FEMS Microbiol Lett 35:183-188. doi: 10.1111/j.1574-6968.1986.tb01524.x.

38. Schurig-Briccio LA, Yano T, Rubin H, Gennis RB. 2014. Characterization of the type 2 NADH:menaquinone oxidoreductases from *Staphylococcus aureus* and the bactericidal action of phenothiazines. Biochim Biophys Acta 1837:954-963. doi: 10.1016/j.bbabio.2014.03.017.

39. Gries CM, Bose JL, Nuxoll AS, Fey PD, Bayles KW. 2013. The Ktr potassium transport system in *Staphylococcus aureus* and its role in cell physiology, antimicrobial resistance and pathogenesis. Mol Microbiol 89:760-773. doi: 10.1111/mmi.12312.

40. Contreras-Moreira B, Vinuesa P. 2013. GET_HOMOLOGUES, a versatile software package for scalable and robust microbial pangenome analysis. Appl Environ Microbiol 79:7696-7701. doi: 10.1128/AEM.02411-13.

41. Epstein W. 1986. Osmoregulation by potassium transport in *Escherichia coli*. FEMS Microbiol Rev 39:73-78. doi: 10.1111/j.1574-6968.1986.tb01845.x.

42. Gründling A. 2013. Potassium uptake systems in *Staphylococcus aureus*: new stories about ancient systems. MBio 4:e00784-13. doi: 10.1128/mBio.00784-13.

43. Fung DK, Lau WY, Chan WT, Yan A. 2013. Copper efflux is induced during anaerobic amino acid limitation in *Escherichia coli* to protect iron-sulfur cluster enzymes and biogenesis. J Bacteriol 195:4556-4568. doi: 10.1128/JB.00543-13.

44. Caby M, Bontemps-Gallo S, Gruau P, Delrue B, Madec E, Lacroix JM. 2018. The EnvZ-OmpR two-component signaling system is inactivated in a mutant devoid of osmoregulated periplasmic glucans in *Dickeya dadantii*. Front Microbiol 9:2459.

45. Li YC, Chang CK, Chang CF, Cheng YH, Fang PJ, Yu T, Chen SC, Li YC, Hsiao CD, Huang TH. 2014. Structural dynamics of the two-component response regulator RstA in recognition of promoter DNA element. Nucleic Acids Res 42:8777-8788. doi: 10.1093/nar/gku572.

46. Freeman ZN, Dorus S, Waterfield NR. 2013. The KdpD/KdpE two-component system: integrating K^+ homeostasis and virulence. PLoS Pathog 9:e1003201. doi: 10.1371/journal.ppat.1003201.

47. Fuchs S, Pané-Farré J, Kohler C, Hecker M, Engelmann S. 2007. Anaerobic gene expression in *Staphylococcus aureus*. J Bacteriol 189:4275-4289. doi: 10.1128/JB.00081-07.

48. Korotetskiy IS, Jumagaziyeva AB, Reva ON, Kuznetsova TV, Shvidko SV, Iskakbayeva ZA, Myrzabayeva AH, Ilin AI. 2019. Isolation and characterization isolates of nosocomial infections. Bul Nat Acad Sci Republic of Kazakhstan 5:199-209. doi: 10.32014/2019.2518-1467.140.

49. Korotetskiy IS, Jumagaziyeva AB, Shilov SV, Kuznetsova TV, Iskakbayeva ZA, Myrzabayeva AH, Korotetskaya NV, Ilin AI, Reva ON. 2020. Phenotypic and genotypic characterisation of clinical isolates of nosocomial infections. Eurasian J Appl Biotechnol 2020:48-60.

50. Baranyi J, Roberts TA. 1994. A dynamic approach to predicting bacterial growth in food. Int J Food Microbiol 23:277-294. doi: 10.1016/0168-1605(94)90157-0.

51. Howden BP, Beaume M, Harrison PF, Hernandez D, Schrenzel J, Seemann T, Francois P, Stinear TP. 2013. Analysis of the small RNA transcriptional response in multidrug-resistant *Staphylococcus aureus* after antimicrobial exposure. Antimicrob Agents Chemother 57:3864-3874. doi: 10.1128/AAC.00263-13.

52. Karp PD, Paley S, Romero P. 2002. The Pathway Tools software. Bioinformatics 18 Suppl 1:S225-232. doi:10.1093/bioinformatics/18.suppl_1.s225.

53. De Maeyer D, Renkens J, Cloots L, De Raedt L, Marchal K. 2013. PheNetic: network-based interpretation of unstructured gene lists in *E. coli*. Mol Biosyst 9:1594-1603. doi: 10.1039/c3mb25551d.

Tables

Table 1. Numbers of regulated genes of three model microorganisms treated with FS-1 in the Lag and Log growth phases.

Strain	**Lag growth phase**		**Log growth phase**	
	Up-regulated	**Down-regulated**	**Up-regulated**	**Down-regulated**
E. coli ATCC BAA-196	42	78	15	43
S. aureus ATCC BAA-39	223	230	76	29
A. baumannii ATCC BAA-1790	102	79	78	127

Figure legends

Fig. 1. Plots of co-regulation of gene in the Lag and Log growth phases. A) *E. coli* BAA-196 (EC_BAA-196_Lag/Log); B) *S. aureus* BAA-39 (SA_BAA-39_Lag/Log); and C) *A. baumannii* BAA-1790 (AB_BAA-1790_Lag/Log). Circles represent protein coding genes (CDS) plotted according to their negative and positive Log_2(fold-change) values calculated in the Log-experiment (axis X) and Lag-experiment (axis Y). The outermost regulated genes are labelled by their names or locus tag numbers. Thin vertical and horizontal lines within the plots separate genes with 2-fold or higher regulation and split the plots into sectors of genes of different categories depending on their coregulation. Numbers of CDS falling to different sectors are shown. Up- and down- coregulated genes, oppositely regulated genes and the genes regulated only in one experiment are depicted by different colours. Statistical reliability of fold change predictions is depicted by sizes of circles as explained in the legend on the bottom part of the figure. Estimated Pearson correlation coefficients are given on the top of each plot.

Fig. 2. Metabolic pathways affected by the treatment of *E. coli* BAA-196 with FS-1 as predicted by analysis of gene regulation in Lag and Log experiments. Up- and down-regulation of metabolic pathways discovered in both, or only in one experiment, are depicted by arrows of different colours and width as explained in the legend on the bottom part of the figure. Cell membrane and cell wall associated proteins are shown by blocks depicted by the same colour scheme. Individual pathways and key compounds are labelled.

Fig. 3. PheNetic network of regulated genes of *E. coli* BAA-196 identified in Lag experiment and clustered according to their regulation by higher level transcriptional regulators. Upregulated genes are depicted by pink nodes and downregulated genes – by green nodes (vertices). Colour intensity indicates the level of expression fold change. Grey nodes are transcriptional regulators involved in the network, which expression was not

reliable changed. Orange edges show regulation by transcriptional activators; and blue edges show regulation by transcriptional repressors. Direct regulations by transcriptional regulators are indicated by arrowheads.

Fig. 4. Metabolic pathways affected by the treatment of *S. aureus* BAA-39 with FS-1 as predicted by analysis of gene regulation in Lag and Log experiments. Up- and down-regulation of metabolic pathways discovered in both, or only in one experiment, are depicted by arrows of different colours and width as explained in the legend on the bottom part of the figure. Cell membrane and cell wall associated proteins are shown by blocks depicted by the same colour scheme. Individual pathways and key compounds are labelled.

Fig. 5. Metabolic pathways affected by the treatment of *A. baumannii* BAA-1790 with FS-1 as predicted by analysis of gene regulation in Lag and Log experiments. Up- and down-regulation of metabolic pathways discovered in both, or only in one experiment, are depicted by arrows of different colours and width as explained in the legend on the bottom part of the figure. Cell membrane and cell wall associated proteins are shown by blocks depicted by the same colour scheme. Individual pathways and key compounds are labelled.

Fig. 6. Plots of co-regulation of homologous gene in the Lag experiment shared by pairs of model microorganisms. A) *E. coli* BAA-196 and *S. aureus* BAA-39 (EC_BAA-196_vs_SA_BAA-39); B) *E. coli* BAA-196 and *A. baumannii* BAA-1790 (EC_BAA-196_vs_ AB_BAA-1790); and C) *S. aureus* BAA-39 and *A. baumannii* BAA-1790 (SA_BAA-39_vs_AB_BAA-1790). Circles represent protein coding genes (CDS) plotted according to their negative and positive Log_2(fold-change) values calculated in the Lag-experiments for different microorganisms shown along axes X and Y. The outermost regulated genes are labelled by their names. Thin vertical and horizontal lines within the plots

separate genes with 2-fold or higher regulation and split the plots to sectors of genes of different categories depending on their coregulation. Numbers of CDS falling to different sectors are shown. Up- and down- coregulated genes, oppositely regulated genes and the genes regulated only in one genome are depicted by different colours. Statistical reliability of fold change predictions is depicted by sizes of the circles as explained in the legend in the bottom part of the figure. Estimated Pearson correlation coefficients are given on the top of each plot.

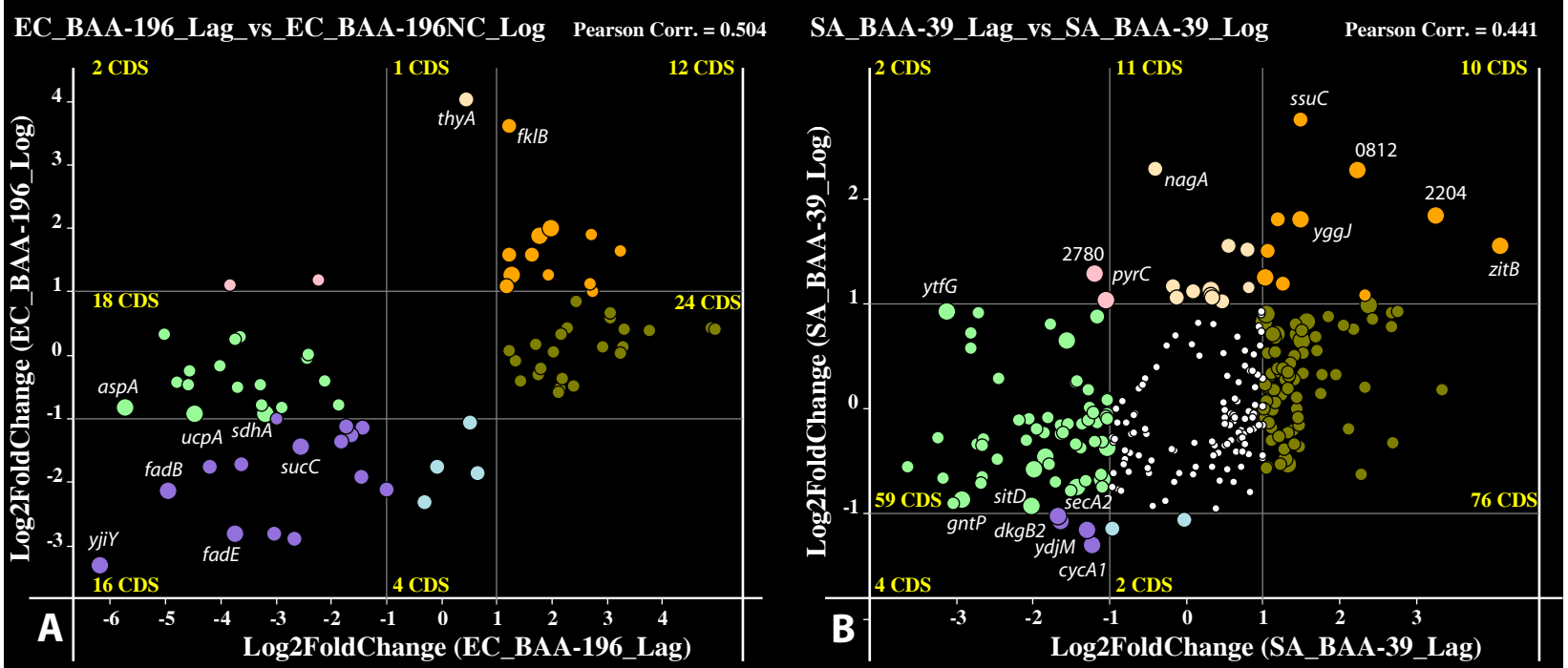

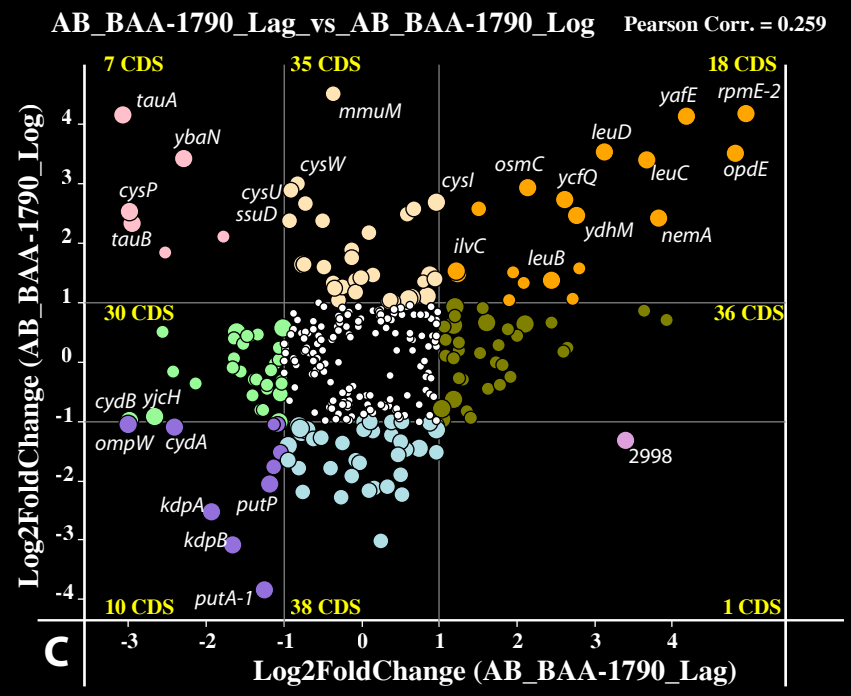

- regulated genes with $p <= 0.05$ in both genomes;
- regulated genes with $p <= 0.05$ in one of two genomes;
- regulated genes with $p > 0.05$ in both genomes;
- non-regulated genes;

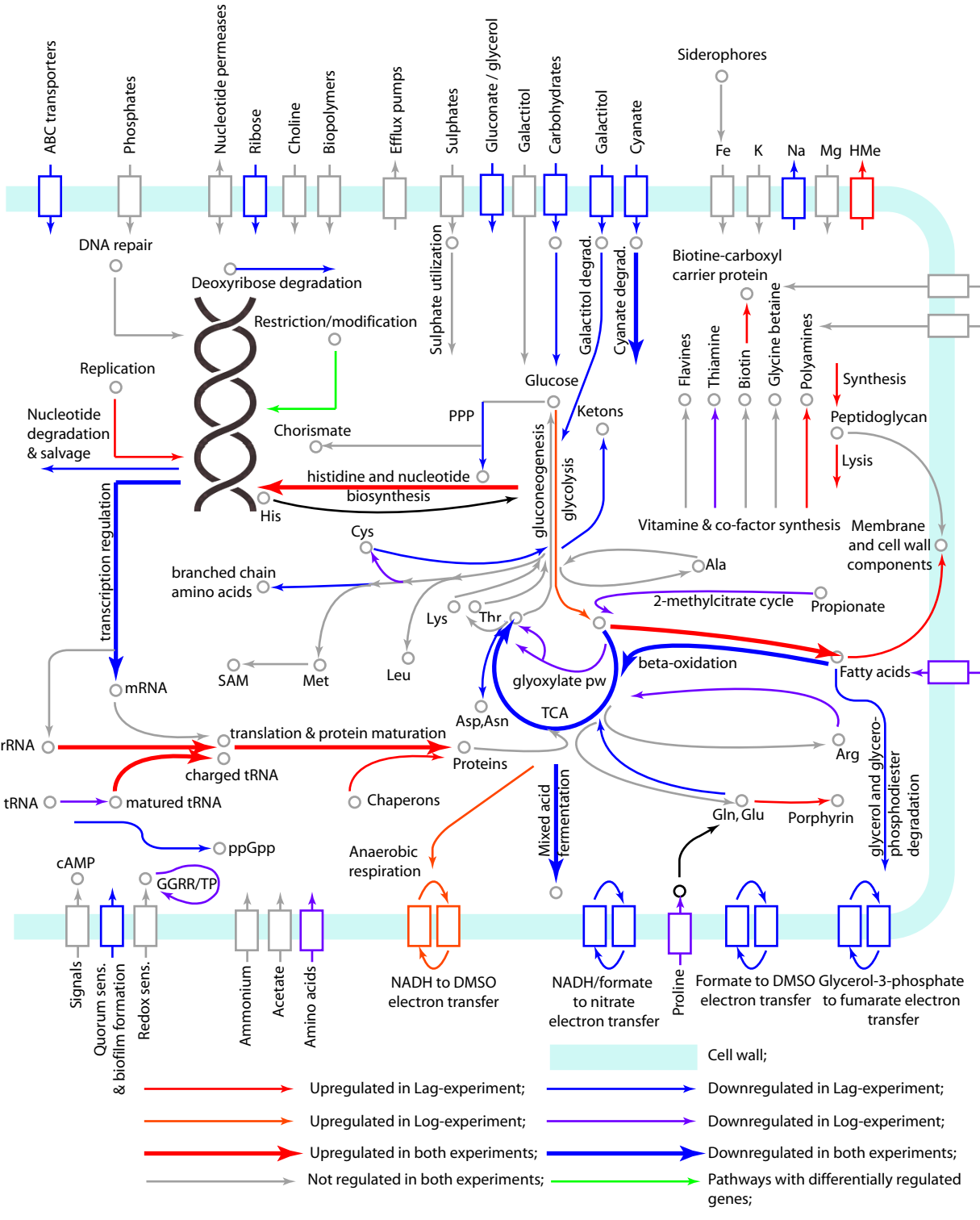
ABC transporters
Phosphates
Nucleotide permeases
Ribose
Choline
Biopolymers
Efflux pumps
Sulphates
Gluconate / glycerol
Galactitol
Carbohydrates
Galactitol
Cyanate
Siderophores
Fe
K
Na
Mg
HMe
DNA repair
Deoxyribose degradation
Restriction/modification
Sulphate utilization
Galactitol degrad.
Cyanate degrad.
Biotine-carboxyl carrier protein
Flavines
Thiamine
Biotin
Glycine betaine
Polyamines
Synthesis
Peptidoglycan
Lysis
Replication
Nucleotide degradation & salvage
Glucose
PPP
Ketons
Chorismate
histidine and nucleotide biosynthesis
His
gluconeogenesis
glycolysis
Vitamine & co-factor synthesis
Membrane and cell wall components
Cys
Ala
branched chain amino acids
2-methylcitrate cycle
Propionate
Lys
Thr
transcription regulation
SAM
Met
Leu
glyoxylate pw
beta-oxidation
Fatty acids
mRNA
Asp,Asn
TCA
rRNA
translation & protein maturation
Proteins
Arg
charged tRNA
tRNA
matured tRNA
Chaperons
Mixed acid fermentation
Gln, Glu
Porphyrin
glycerol and glycero-phosphodiester degradation
ppGpp
cAMP
GGRR/TP
Anaerobic respiration
Signals
Quorum sens. & biofilm formation
Redox sens.
Ammonium
Acetate
Amino acids
NADH to DMSO electron transfer
NADH/formate to nitrate electron transfer
Proline
Formate to DMSO electron transfer
Glycerol-3-phosphate to fumarate electron transfer
Cell wall;
Upregulated in Lag-experiment;
Downregulated in Lag-experiment;
Upregulated in Log-experiment;
Downregulated in Log-experiment;
Upregulated in both experiments;
Downregulated in both experiments;
Not regulated in both experiments;
Pathways with differentially regulated genes;

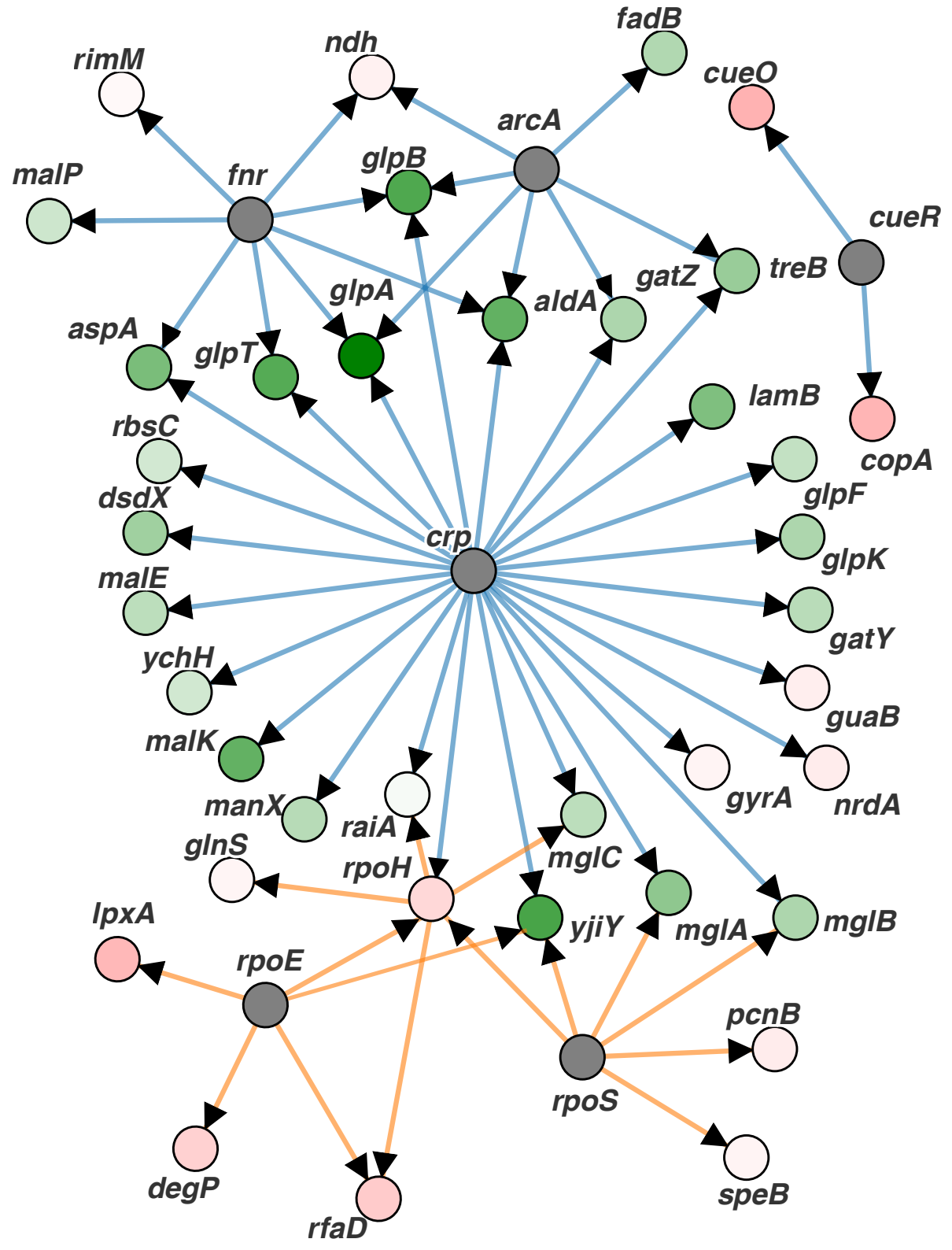
fadB
ndh
rimM
cueO
arcA
glpB
malP
fnr
cueR
treB
gatZ
aldA
glpA
aspA
glpT
lamB
rbsC
copA
glpF
dsdX
crp
glpK
malE
gatY
ychH
guaB
malK
gyrA
nrdA
manX
raiA
mglC
glnS
rpoH
lpxA
yjiY
mglA
mglB
rpoE
pcnB
rpoS
degP
speB
rfaD

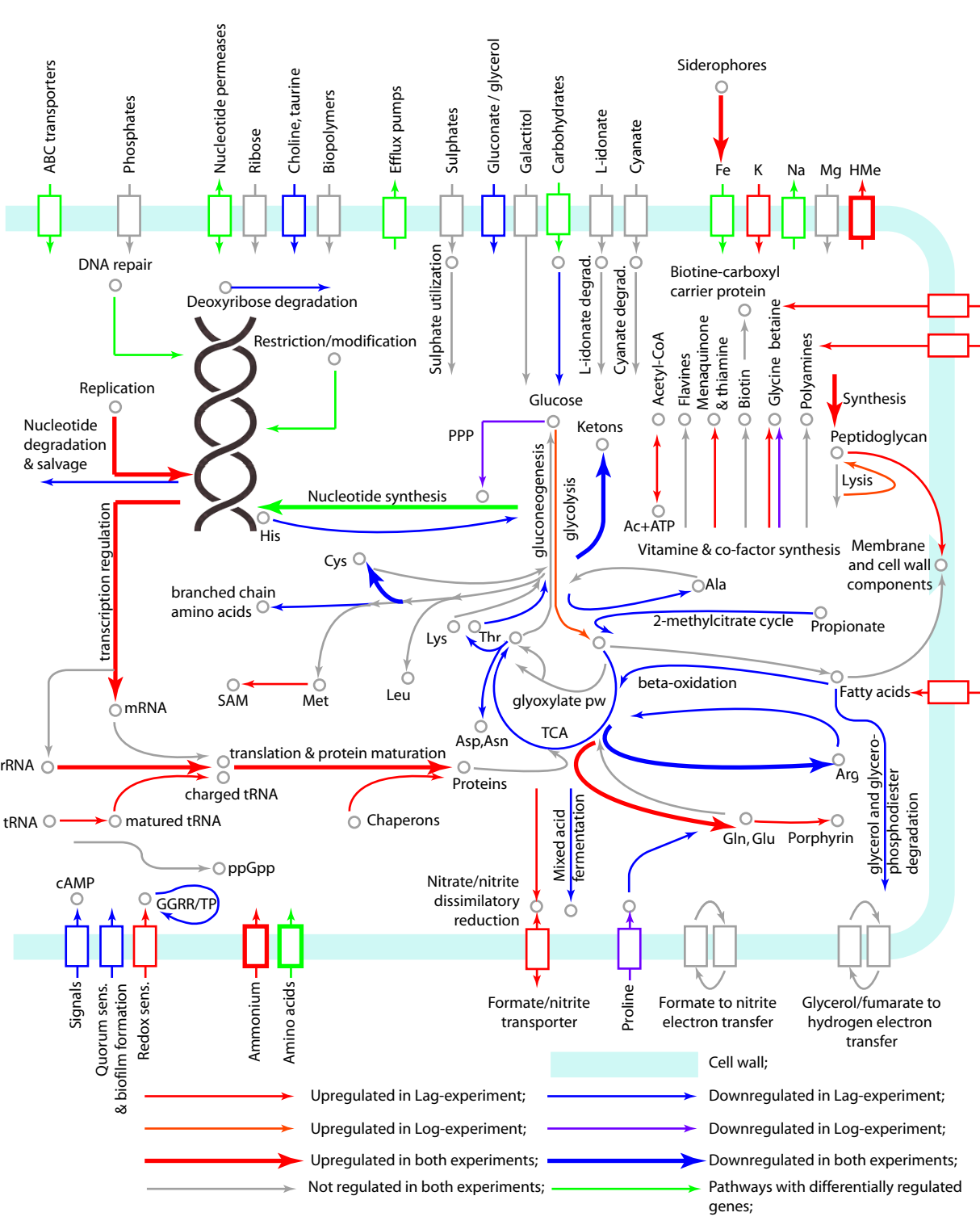
ABC transporters
Phosphates
Nucleotide permeases
Ribose
Choline, taurine
Biopolymers
Efflux pumps
Sulphates
Gluconate / glycerol
Galactitol
Carbohydrates
L-idonate
Cyanate
Siderophores
Fe
K
Na
Mg
HMe
DNA repair
Deoxyribose degradation
Restriction/modification
Replication
Nucleotide degradation & salvage
Sulphate utilization
L-idonate degrad.
Cyanate degrad.
Biotine-carboxyl carrier protein
Glycine betaine
Polyamines
Synthesis
Peptidoglycan
Lysis
Acetyl-CoA
Flavines
Menaquinone & thiamine
Biotin
Glucose
Ketons
PPP
gluconeogenesis
glycolysis
Nucleotide synthesis
His
Ac+ATP
Vitamine & co-factor synthesis
Membrane and cell wall components
Cys
Ala
branched chain amino acids
2-methylcitrate cycle
Propionate
Lys
Thr
transcription regulation
SAM
Met
Leu
glyoxylate pw
TCA
beta-oxidation
Fatty acids
mRNA
Asp,Asn
rRNA
translation & protein maturation
Proteins
Arg
charged tRNA
tRNA
matured tRNA
Chaperons
Gln, Glu
Porphyrin
glycerol and glycero-phosphodiester degradation
ppGpp
cAMP
GGRR/TP
Nitrate/nitrite dissimilatory reduction
Mixed acid fermentation
Signals
Quorum sens. & biofilm formation
Redox sens.
Ammonium
Amino acids
Formate/nitrite transporter
Proline
Formate to nitrite electron transfer
Glycerol/fumarate to hydrogen electron transfer
Cell wall;
Upregulated in Lag-experiment;
Downregulated in Lag-experiment;
Upregulated in Log-experiment;
Downregulated in Log-experiment;
Upregulated in both experiments;
Downregulated in both experiments;
Not regulated in both experiments;
Pathways with differentially regulated genes;

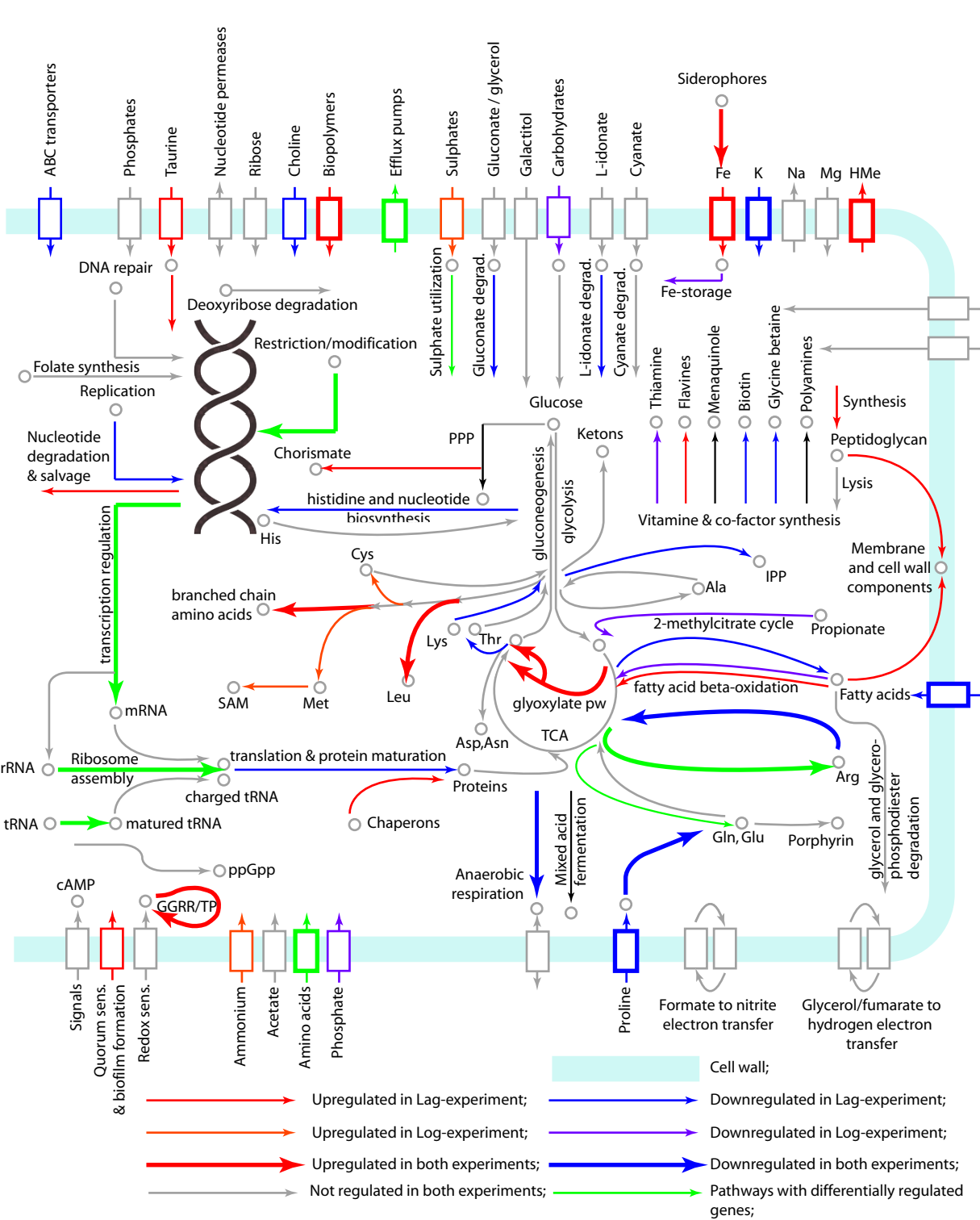
ABC transporters
Phosphates
Taurine
Nucleotide permeases
Ribose
Choline
Biopolymers
Efflux pumps
Sulphates
Gluconate / glycerol
Galactitol
Carbohydrates
L-idonate
Cyanate
Siderophores
Fe
K
Na
Mg
HMe
DNA repair
Deoxyribose degradation
Restriction/modification
Folate synthesis
Replication
Nucleotide degradation & salvage
Chorismate
PPP
Sulphate utilization
Gluconate degrad.
L-idonate degrad.
Cyanate degrad.
Fe-storage
Glucose
Ketons
Thiamine
Flavines
Menaquinole
Biotin
Glycine betaine
Polyamines
Synthesis
Peptidoglycan
Lysis
Vitamine & co-factor synthesis
histidine and nucleotide biosynthesis
His
gluconeogenesis
glycolysis
transcription regulation
Cys
IPP
Ala
Membrane and cell wall components
branched chain amino acids
Lys
Thr
2-methylcitrate cycle
Propionate
SAM
Met
Leu
glyoxylate pw
fatty acid beta-oxidation
Fatty acids
mRNA
Asp,Asn
TCA
rRNA
Ribosome assembly
translation & protein maturation
Proteins
Arg
charged tRNA
tRNA
matured tRNA
Chaperons
Gln, Glu
Porphyrin
glycerol and glycero-phosphodiester degradation
ppGpp
cAMP
GGRR/TP
Anaerobic respiration
Mixed acid fermentation
Signals
Quorum sens. & biofilm formation
Redox sens.
Ammonium
Acetate
Amino acids
Phosphate
Proline
Formate to nitrite electron transfer
Glycerol/fumarate to hydrogen electron transfer
Cell wall;
Upregulated in Lag-experiment;
Downregulated in Lag-experiment;
Upregulated in Log-experiment;
Downregulated in Log-experiment;
Upregulated in both experiments;
Downregulated in both experiments;
Not regulated in both experiments;
Pathways with differentially regulated genes;

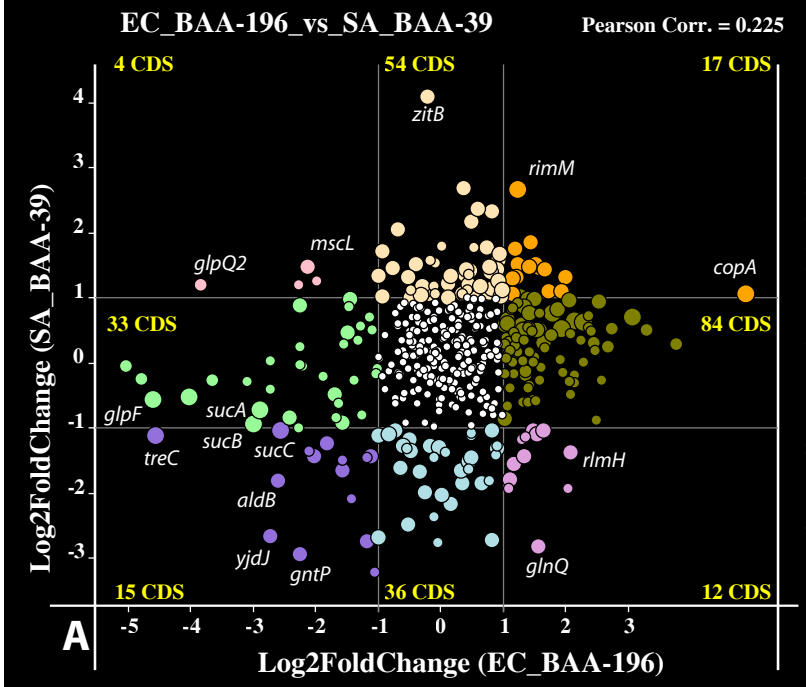

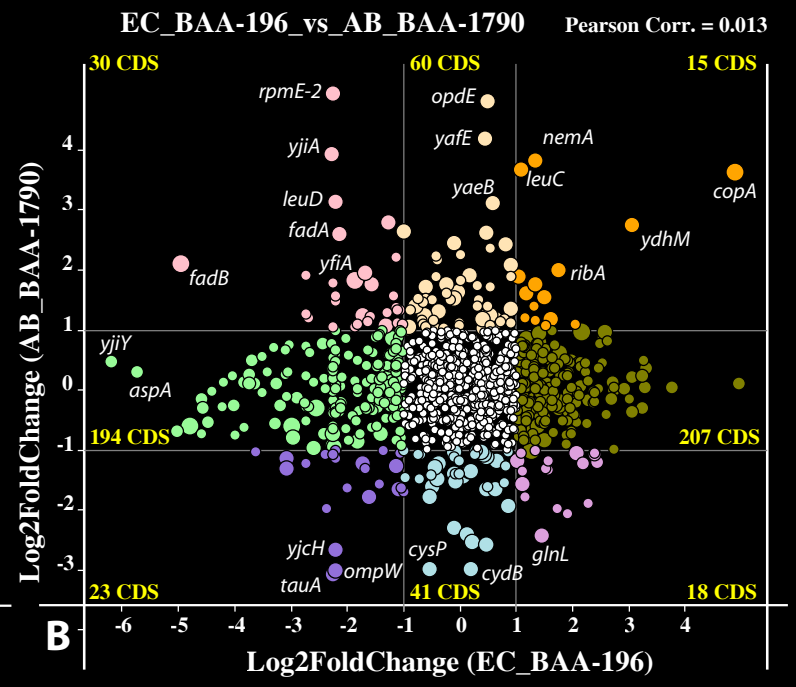

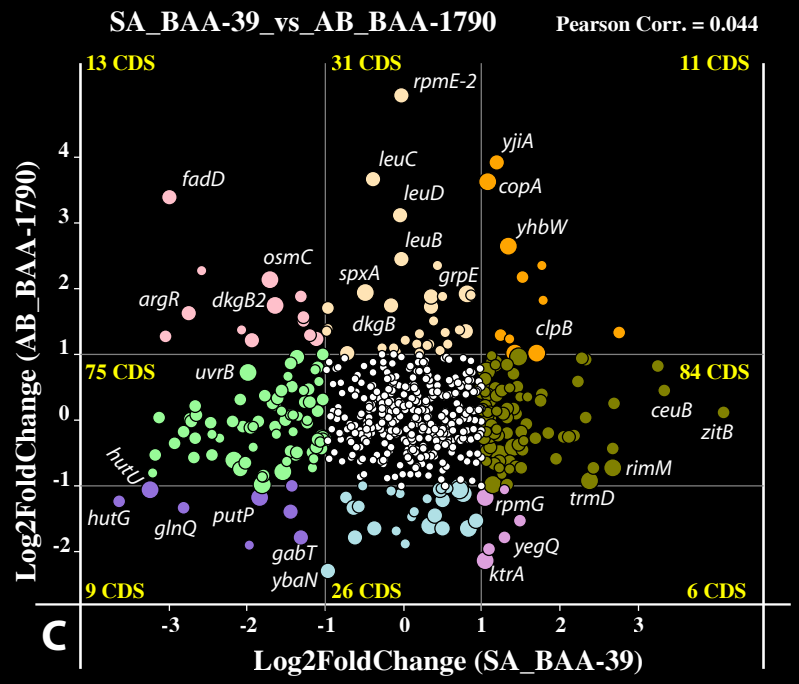

● - regulated genes with $p <= 0.05$ in both genomes;

● - regulated genes with $p <= 0.05$ in one of two genomes;

• - regulated genes with $p > 0.05$ in both genomes;

• - non-regulated genes shared by both genomes;